Available online at www.sciencedirect.com
SCIENCE DIRECT®
Biochemical and Biophysical Research Communications 316 (2004) 636–642
BBRC
www.elsevier.com/locate/ybbrc

Modelling extracellular domains of GABA-A receptors: subtypes 1, 2, 3, and 5

Kuo-Chen Chou*

Tianjin Institute of Bioinformatics and Drug Discovery (TIBDD), Tianjin 300074, China
Life Science Research Center, Shanghai Jiaotong University, Shanghai 200030, China

Received 13 February 2004

Abstract

GABA is the main inhibitory neurotransmitter in the mammalian central nervous system. When GABA binds to the ubiquitous GABA-A receptors on neurons, chloride channels are activated leading to a rapid increase in chloride conductance that depresses excitatory depolarization. The GABA-A receptors are targets for many clinically important drugs, such as the benzodiazepines, general anaesthetics, and barbiturates. All of these drugs enhance the chloride current activated by GABA. Of the GABA-A receptor family, the subtype 2 is critical for the treatment of anxiety spectrum disorders. To avoid unwanted side effects, it is necessary to find highly selective drugs that interact only with subtype 2 but not with the related receptors such as subtypes 1, 3, and 5. To realize such a goal, it is important to have not only the 3D (dimensional) structure of subtype 2 but also the 3D structures of subtypes 1, 3, and 5. In this study, the 3D structures of all the four subtypes of GABA-A receptors have been derived. The computer-modeled heteropentameric structures bear the following features: (1) each of the five subunits in the pentamer has an intrachain disulfide bond, a hallmark of ligand-gated pentameric channels; (2) those residues which are sensitive to the binding of the benzodiazepine site ligands are grouped around the $\alpha_{1,2,3,5}/\gamma_2$ interfaces; and (3) those residues which are sensitive to the binding of GABA molecules are grouped around the $\alpha_{1,2,3,5}/\beta_2$ interfaces. All these findings are fully consistent with experimental observations. Meanwhile, for those sensitive or key residues, a close look at their subtle difference among the four subtypes has been provided through a highlighted superposition picture. In addition to providing the atomic coordinates, the predicted structures have further clarified some ambiguities that could not been uniquely determined by the existing experimental data, such as the directionality of the subunit arrangement in the heteropentamers. The 3D models may provide a reasonable structural frame or footing for designing highly selective drugs. The present models might be also useful in understanding the basic mechanism of operation of the GABA-A receptors, stimulating novel strategies for developing more specific drugs and better treatments.

Keywords: Benzodiazepine pharmacology; GABAergic inhibition; $\alpha_{1,2,3,5}/\beta_2$ interfaces; $\alpha_{1,2,3,5}/\gamma_2$ interfaces; Benzodiazepine binding site; Ligand-gated chloride channel; Directionality of heteropentamer

Several amino acids have distinct excitatory or inhibitory effects upon the nervous system. As an amino acid derivative, GABA (γ-aminobutyric acid) is the most important and abundant inhibitory neurotransmitter in the brain. Acting as a "balancer," it helps induce relaxation and sleep by balancing excitation of the brain with inhibition. The formation of GABA occurs by the decarboxylation of glutamate catalyzed by GAD (glutamate decarboxylase). The enzyme is present in many nerve endings of the brain as well as in the β-cells of the pancreas. Neurons that secrete GABA are termed GABAergic. GABA exerts its effects by binding to two distinct receptors, GABA-A and GABA-B. The GABA-A receptors are pentameric membrane proteins that operate as GABA-gated Cl^- channels responsible for synaptic inhibition. The anxiolytic drugs of the benzodiazepine family exert their soothing effects by potentiating the responses of GABA-A receptors to GABA binding. The GABA-B receptors are coupled to an intracellular G-protein and act by increasing conductance of an associated K^+ channel. The present studies are focused on GABA-A receptors.

* Fax: +86-22-2335-8494.
E-mail address: kchou@san.rr.com.

0006-291X/$ - see front matter © 2004 Elsevier Inc. All rights reserved.
doi:10.1016/j.bbrc.2004.02.098

GABA-A receptors exhibit varied structural heterogeneity and are assembled from a repertoire of at least 18 subunits. These receptors are most clearly distinguished by their subunit architecture, which in mammalian brain comprises seven different classes of subunits with multiple variants (α_{1-6}, β_{1-3}, γ_{1-3}, δ, ε, ϑ, and ρ_{1-3}). Most GABA-A receptor subtypes in vivo are believed to be composed of α, β, and γ subunits. Of the 12 constituent subunits (α_{1-6}, β_{1-3}, and γ_{1-3}), β_2 is ubiquitous and the most abundant subunit in the brain. And γ_2 is a necessary subunit for benzodiazepine binding [1]. For the six α isoforms, only α_1, α_2, α_3, and α_5 determine benzodiazepine pharmacology. This is because the residue His-129 of α_1 (or the equivalent His at α_2, α_3, and α_5) is critical for benzodiazepine binding [2]. The equivalent position at α_4 and α_6 is occupied by Arg and its mutation to His is required for their interaction with classical benzodiazepines. Accordingly, despite numerous possible $\alpha\beta\gamma$ combinations, $\alpha_k\beta_2\gamma_2$ ($k = 1$, 2, 3, and 5) combinations, or subtypes 1, 2, 3, and 5, appear to be prototypic for GABA-A receptors, sharing many properties with those of native neuronal receptors. Of the four receptors, subtype 1 is thought to be the most abundant in the adult brain [3]. On the other hand, it has been shown by mounting evidence that the subtype 2 is critical for mediating the anxiolysis produced by classical benzodiazepines. Acting by enhancing the GABA-A receptor function in the central nervous system, classical benzodiazepine drugs are in wide clinical use as anxiolytics, hypnotics, anticonvulsants, and muscle relaxants [4]. To stimulate the structure-based design for new drugs that target restricted neuronal networks and minimize side effects, it is vitally important to find the 3D structures of GABA-A receptors in all the relevant subtypes. The present study was initiated in an attempt to find the 3D structures for the ectodomains of subtypes 1, 2, 3, and 5, respectively.

Materials and methods

In the existing literature, the symbols for the subtypes 1, 2, 3, and 5 of GABA-A receptors are usually denoted by $\alpha_1\beta_2\gamma_2$, $\alpha_2\beta_2\gamma_2$, $\alpha_3\beta_2\gamma_2$, and $\alpha_5\beta_2\gamma_2$, respectively. Since they are heteropentameric membrane proteins in which the C-terminals of the five subunits are located in the cytoplasmic side and their N-terminals at the extracellular side, the existing representations would lack uniqueness. To clarify the ambiguity, here let us propose the following symbol to uniquely express their stoichiometry and subunit arrangement [5–7]. As shown in Fig. 1, the subunits S_1, S_2, S_3, S_4, and S_5 follow a clockwise order arrangement when viewed from C- to N-terminal, or from the cytoplasmic to the extracellular side. However, according to the existing experimental data a corresponding mirror image subunit arrangement is equally possible [8], implying that the directionality could not be uniquely defined. In other words, if the pentamer of Fig. 1 is formulated by

$$\overrightarrow{S_1S_2S_3S_4S_5}(C \to N) \tag{1}$$

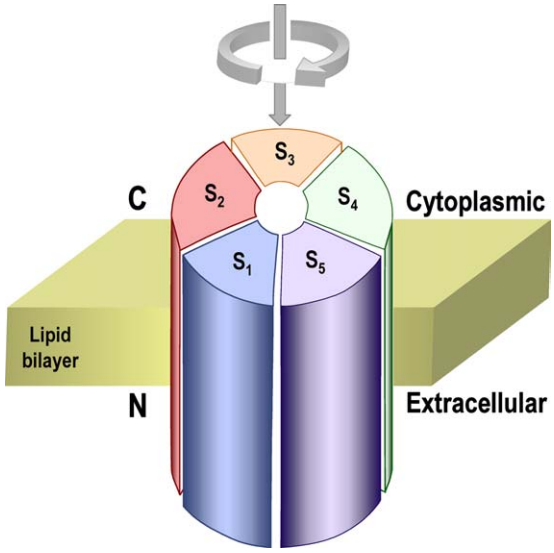

Fig. 1. Schematic drawing to show the stoichiometry and the arrangement of the five subunits in a GABA-A receptor, with a view from C- to N-terminal. According to the existing experimental data, a mirror image subunit arrangement is equally possible [8]. The 3D model derived from this study can help clarify such an ambiguity and uniquely define the arrangement. See Eqs. (1)–(4) and the relevant text for further explanation.

where the subunits follow a clockwise order arrangement when viewed from C- to N-terminal, then its mirror image will be formulated by

$$\underleftarrow{S_1S_2S_3S_4S_5}(C \to N) \tag{2}$$

where the corresponding subunits will follow a counterclockwise order arrangement as indicated by the underlying arrow bar. Therefore, before the issue regarding the possible two arrangements can be solved, subtypes 1, 2, 3, and 5 of $GABA_A$ receptors may be expressed as either (clockwise)

$$\begin{cases} \overrightarrow{\alpha_1\beta_2\alpha_1\gamma_2\beta_2}(C \to N) & \text{for subtype 1} \\ \overrightarrow{\alpha_2\beta_2\alpha_2\gamma_2\beta_2}(C \to N) & \text{for subtype 2} \\ \overrightarrow{\alpha_3\beta_2\alpha_3\gamma_2\beta_2}(C \to N) & \text{for subtype 3} \\ \overrightarrow{\alpha_5\beta_2\alpha_5\gamma_2\beta_2}(C \to N) & \text{for subtype 5} \end{cases} \tag{3}$$

or (counterclockwise)

$$\begin{cases} \overleftarrow{\alpha_1\beta_2\alpha_1\gamma_2\beta_2}(C \to N) & \text{for subtype 1} \\ \overleftarrow{\alpha_2\beta_2\alpha_2\gamma_2\beta_2}(C \to N) & \text{for subtype 2} \\ \overleftarrow{\alpha_3\beta_2\alpha_3\gamma_2\beta_2}(C \to N) & \text{for subtype 3} \\ \overleftarrow{\alpha_5\beta_2\alpha_5\gamma_2\beta_2}(C \to N) & \text{for subtype 5} \end{cases} \tag{4}$$

The sequences of α_1, α_2, α_3, α_5, β_2, and γ_2 subunits for the four human GABA-A receptors studied here were taken from [9–13]. The numbers of total residues for α_1, α_2, α_3, α_5, β_2, and γ_2 subunits are 456, 451, 492, 462, 474, and 467, respectively. The sequence locations in different domains for each of the six subunits are given by

$$\begin{cases} \alpha_1: & 1\text{–}27 \text{ (signal)}; & 28\text{–}251 \text{ (extracellular)}; & 252\text{–}456 \text{ (intracellular)} \\ \alpha_2: & 1\text{–}28 \text{ (signal)}; & 29\text{–}251 \text{ (extracellular)}; & 252\text{–}451 \text{ (intracellular)} \\ \alpha_3: & 1\text{–}28 \text{ (signal)}; & 29\text{–}276 \text{ (extracellular)}; & 277\text{–}492 \text{ (intracellular)} \\ \alpha_5: & 1\text{–}31 \text{ (signal)}; & 32\text{–}258 \text{ (extracellular)}; & 259\text{–}462 \text{ (intracellular)} \\ \beta_2: & 1\text{–}24 \text{ (signal)}; & 25\text{–}244 \text{ (extracellular)}; & 245\text{–}474 \text{ (intracellular)} \\ \gamma_2: & 1\text{–}39 \text{ (signal)}; & 40\text{–}273 \text{ (extracellular)}; & 274\text{–}467 \text{ (intracellular)} \end{cases} \tag{5}$$

where the sequence positions in different domains were obtained either directly from [9–13] or derived by a bioinformatic analysis (see, e.g., [14,15]). For the current study, the signal peptide segments were not included because they will be cleaved off by signal peptidase during the secretory process (see, e.g., [16]). Also the intracellular domains need not be considered here since they are outside of the benzodiazepine binding site. Accordingly, our target should be focused on the extracellular domains.

Since molluscan AChBP (acetylcholine-binding protein) is a structural and functional homologue of the amino-terminal ligand-binding domain of a GABA-A receptor [17], the crystal structure of AChBP (1i9b.pdb) could be used as a template for the current prediction. The relevant sequence alignment was performed using the CLUSTALW [14]. The aligned result is shown in Fig. 2, where only one chain of AChBP (abbreviated as 1i9b) is shown due to the fact that AChBP is a homopentamer. According to the alignment of Fig. 2, the 3D model of the $\overrightarrow{\boldsymbol{\alpha}_1\boldsymbol{\beta}_2\boldsymbol{\alpha}_1\boldsymbol{\gamma}_2\boldsymbol{\beta}_2}(\mathrm{C} \rightarrow \mathrm{N})$ was constructed through the following five steps. (1) Generate the $\boldsymbol{\alpha}_1$ subunit based on the 1st chain of 1i9b.pdb with the presence of its other four chains as an environment. (2) Generate the $\boldsymbol{\beta}_2$ subunit based on the 2nd chain of 1i9b.pdb with the presence of the new-generated $\boldsymbol{\alpha}_1$ subunit as well as the chains 3–5 of 1i9b.pdb as an environment. (3) Generate the second $\boldsymbol{\alpha}_1$ subunit based on the 3rd chain of 1i9b.pdb with the presence of the two subunits generated in steps 1–2 as well as the chains 4–5 of 1i9b.pdb. (4) Generate the $\boldsymbol{\gamma}_2$ subunit based on the 4th chain of 1i9b.pdb with the presence of the three subunits generated in steps 1–3 as well as the chains 5 of 1i9b.pdb. (5) Generate the second $\boldsymbol{\beta}_2$ subunit based on the 5th chain of 1i9b.pdb with the presence of the four subunits generated in steps 1–4. The presence of the other chains during the modeling process as described in the above steps is important in order to avoid the formation of any conflicting structure with overlap or penetration. Obviously, during the above steps if the order for generating the second $\boldsymbol{\alpha}_1$ subunit and $\boldsymbol{\gamma}_2$ subunit was reversed, then the heteropentamer thus obtained would be $\underrightarrow{\boldsymbol{\alpha}_1\boldsymbol{\beta}_2\boldsymbol{\alpha}_1\boldsymbol{\gamma}_2\boldsymbol{\beta}_2}(\mathrm{C} \rightarrow \mathrm{N})$, which just has an opposite direction to $\overrightarrow{\boldsymbol{\alpha}_1\boldsymbol{\beta}_2\boldsymbol{\alpha}_1\boldsymbol{\gamma}_2\boldsymbol{\beta}_2}(\mathrm{C} \rightarrow \mathrm{N})$ (see Eqs. (3) and (4)). During the above operation, each of the subunit chains was computed by using the segment matching modeling method, in which a database of known protein structures was employed to build an unknown target structure-based on an amino acid sequence alignment [18–22]. In the current case the target structure was each of the subunits in a heteropentamer that are to be predicted. The modeling operation consisted of the following procedures: (a) the target chain was first broken into short segments of sequence; (b) the database (formed by more than 5200 high-resolution X-ray protein structures) was searched for matching segments according to the sequence alignment and the shape of the template protein chain; (c) these segment coordinates were fitted into the growing target structure under the monitor to avoid any van der Waal overlap until all atomic coordinates of the target structure were obtained; and (d) the process was repeated 10 times and an average model was generated, followed by energy minimization of the entire chain with the presence of the corresponding other four chains as an environment as described in the above steps 1–5.

Finally, the five chains thus generated were subjected to an overall energy minimization with respect to all the atoms to create the final 3D models for $\overrightarrow{\boldsymbol{\alpha}_1\boldsymbol{\beta}_2\boldsymbol{\alpha}_1\boldsymbol{\gamma}_2\boldsymbol{\beta}_2}(\mathrm{C} \rightarrow \mathrm{N})$ and $\underrightarrow{\boldsymbol{\alpha}_1\boldsymbol{\beta}_2\boldsymbol{\alpha}_1\boldsymbol{\gamma}_2\boldsymbol{\beta}_2}(\mathrm{C} \rightarrow \mathrm{N})$, respectively.

By following the similar procedures, the 3D structures for $\overrightarrow{\boldsymbol{\alpha}_2\boldsymbol{\beta}_2\boldsymbol{\alpha}_2\boldsymbol{\gamma}_2\boldsymbol{\beta}_2}(\mathrm{C} \rightarrow \mathrm{N})$ and $\underrightarrow{\boldsymbol{\alpha}_2\boldsymbol{\beta}_2\boldsymbol{\alpha}_2\boldsymbol{\gamma}_2\boldsymbol{\beta}_2}(\mathrm{C} \rightarrow \mathrm{N})$, $\overrightarrow{\boldsymbol{\alpha}_3\boldsymbol{\beta}_2\boldsymbol{\alpha}_3\boldsymbol{\gamma}_2\boldsymbol{\beta}_2}(\mathrm{C} \rightarrow \mathrm{N})$ and $\underrightarrow{\boldsymbol{\alpha}_3\boldsymbol{\beta}_2\boldsymbol{\alpha}_3\boldsymbol{\gamma}_2\boldsymbol{\beta}_2}(\mathrm{C} \rightarrow \mathrm{N})$, as well as $\overrightarrow{\boldsymbol{\alpha}_5\boldsymbol{\beta}_2\boldsymbol{\alpha}_5\boldsymbol{\gamma}_2\boldsymbol{\beta}_2}(\mathrm{C} \rightarrow \mathrm{N})$ and $\underrightarrow{\boldsymbol{\alpha}_5\boldsymbol{\beta}_2\boldsymbol{\alpha}_5\boldsymbol{\gamma}_2\boldsymbol{\beta}_2}(\mathrm{C} \rightarrow \mathrm{N})$ were also derived.

The segment matching approach was previously used to model the structure of the protease domain of caspase-8, at a time before the X-ray coordinates were released for caspase-3 [23]. In that particular study, the atomic coordinates of the catalytic domain of caspase-3 were predicted based on the X-ray structure of caspase-1, and then the caspase-3 structure thus obtained served as a template to model the protease domain of caspase-8. After the X-ray coordinates of caspase-3 protease domain were finally released and the X-ray structure of the caspase-8

```
                                  28
α1      .......... .......... ....QPSLQ. DELKDNTTVF T.........
                                    29
α2      .......... .......... ......NIQE DEAKNNITIF T.........
        29
α3      QGESRRQEPG DFVKQDIGGL SPKHAPDIP. DDSTDNITIF T.........
                                32
α5      .......... .......... ..QMPTSSVK DETNDNITIF T.........
                                   25
β2      .......... .......... .....QSVN. DPSNMSLVKE T.........
                                40
γ2      .......... .......... ..QKSDDDYE DYASNKTWVL TPKVPEGDVT
                                            8
1I9B    .......... .......... .......... ...FDRADIL Y.........

                                                            92
α1      RILDRLLDGY DNRLRPGLGE RVTEVKTDIF VTSFGPVSDH DMEYTIDVFF
                                                            92
α2      RILDRLLDGY DNRLRPGLGD SITEVFTNIY VTSFGPVSDT DMEYTIDVFF
                                                            117
α3      RILDRLLDGY DNRLRPGLGD AVTEVKTDIY VTSFGPVSDT DMEYTIDVFF
                                                            99
α5      RILDGLLDGY DNRLRPGLGE RITQVRTDIY VTSFGPVSDT EMEYTIDVFF
β2      ..VDRLLKGY DIRLRPDFGG PPVAVGMNID IASIDMVSEV NMDYTLTMYF
                                      96                    116
γ2      VILNNLLEGY DNKLRPDIGV KPTLIHTDMY VNSIGPVNAI NMEYTIDIFF
1I9B    ..NIRQTSRP D..VIPTQRD RPVAVSVSLK FINILEVNEI TNEVDVVFWQ
                                              129
α1      RQSWKDERLK FKGPMTVLRL NNLMASKIRT PDTFFHNGKK SVAHNMTMPN
                                              129
α2      RQKWKDERLK FKGPMNILRL NNLMASKIWT PDTFFHNGKK SVAHNMTMPN
                                              154
α3      RQTWHDERLK FDGPMKILPL NNLLASKIWT PDTFFHNGKK SVAHNMTTPN
                                              136
α5      RQSWKDERLR FKGPMQRLPL NNLLASKIWT PDTFFHNGKK SIAHNMTTPN
β2      QQAWRDKRLS YNVIPLNLTL DNRVADQLWV PDTYFLNDKK SFVHGVTVKN
                                   143
γ2      AQMWYDRRLK FNSTIKVLRL NSNMVGKIWI PDTFFRNSKK ADAHWITTPN
1I9B    QTTWSDRTLA WNSSHSPDQV SVPISS.LWV PDLAAYNAIS ..KPEVLTP.
           147                  166            180     187
α1      KLLRITEDGT LLYTMRLTVR AECPMHLEDF PMDAHACPLK FGSYAYTRAE
           147                  166            180     187
α2      KLLRIQDDGT LLYTMRLTVQ AECPMHLEDF PMDAHSCPLK FGSYAYTTSE
           172                  191            205     212
α3      KLLRLVDNGT LLYTMRLTIH AECPMHLEDF PMDVHACPLK FGSYAYTTAE
           154                  173            187     194
α5      KLLRLEDDGT LLYTMRLTIS AECPMQLEDF PMDAHACPLK FGSYAYPNSE
                                160            174     181 184
β2      RMIRLHPDGT VLYGLRITTT AACMMDLRRY PLDEQNCTLE IESYGYTTDD
         169          181       190            204
γ2      RMLRIWNDGR VLYSLRLTID AECQLQLHNF PMDEHSCPLE FSSYGYPREE
                                130            143
1I9B    QLARVVSDGE VLYMPSIRQR FSCDVSGVDT ESGA.TCRIK IGSWTHHSRE
                                               228    234 237
α1      VVYEWTREPA RSVVVAEDGS .RLNQYDLLG QTV.DSGIVQ SSTGEYVVMT
                                               228    234 237
α2      VTYIWTYNAS DSVQVAPDGS .RLNQYDLLG QSI.GKETIK SSTGEYTVMT
                                               253    259 262
α3      VVYSWTLGKN KSVEVAQDGS .RLNQYDLLG HVV.GTEIIR SSTGEYVVMT
                                               235    241 244
α5      VVYVWTNGST KSVVVAEDGS .RLNQYHLMG QTV.GTENIS TSTGEYTIMT
                                                      226 229
β2      IEFYWRGDD. .NAVTGVTKI .ELPQFSIVD YKL.ITKKVV FSTGSYPRLS
γ2      IVYQWKR.S. .SVEVGDTRS WRLYQFSFVG LRN.TTEVVK TTSGDYVVMS
1I9B    ISVDPTTENS DDSEYFSQYS .RFEILDVTQ KKNSVTYSCC PEAYEDVEVS

                   251
α1      THFHLK.R.K IG.
                   251
α2      AHFHLK.R.K IG.
                   276
α3      THFHLK.R.K IG.
                   258
α5      AHFHLK.R.K IG.
                     244
β2      LSFKLK.R.N IGY
                   273
γ2      VYFDLS.R.R MG.
                   217
1I9B    LNFRKKGRSE IL.
```

Fig. 2. The multiple sequence alignment between 1i9b (one chain of the AChBP homopentamer) and $\boldsymbol{\alpha}_1$, $\boldsymbol{\alpha}_2$, $\boldsymbol{\alpha}_3$, $\boldsymbol{\alpha}_5$, $\boldsymbol{\beta}_2$, and $\boldsymbol{\gamma}_2$ subunits of GABA-A receptor heteropentamer. The codes in boldface type represent the residues known important to ligand binding. See Eq. (5) and the relevant text for further explanation.

protease domain was determined [24], it turned out that the RMSD (root-mean-square-deviation) for all the backbone atoms of the caspase-3 protease domain between the X-ray and predicted structures was 2.7 Å, while the corresponding RMSD was 3.1 Å for caspase-8 and only 1.2 Å for its core structure. This indicates that the computed structures of caspase-3 and -8 were quite close to the corresponding X-ray structures. Later on, this method was successively applied to model the CARDs (caspase recruitment domains) of Apaf-1, Ced-4, and Ced-3, based on the NMR structure of the RAIDD CARD [25], and to model the Cdk5-P35 complex [26] as well as the protease domain of caspase-9 [27]. Recently, it was also used to model the tertiary structure of β-secretase zymogen successfully elucidating the experimental observations that the prodomain of β-secretase does not suppress activity as in a strict zymogen [28].

Results and discussion

Let us first examine the structures as formulated by Eq. (3), i.e., $\overrightarrow{\boldsymbol{\alpha}_1\boldsymbol{\beta}_2\boldsymbol{\alpha}_1\boldsymbol{\gamma}_2\boldsymbol{\beta}_2}(\mathrm{C}\rightarrow\mathrm{N})$, $\overrightarrow{\boldsymbol{\alpha}_2\boldsymbol{\beta}_2\boldsymbol{\alpha}_2\boldsymbol{\gamma}_2\boldsymbol{\beta}_2}(\mathrm{C}\rightarrow\mathrm{N})$, $\overrightarrow{\boldsymbol{\alpha}_3\boldsymbol{\beta}_2\boldsymbol{\alpha}_3\boldsymbol{\gamma}_2\boldsymbol{\beta}_2}(\mathrm{C}\rightarrow\mathrm{N})$, and $\overrightarrow{\boldsymbol{\alpha}_5\boldsymbol{\beta}_2\boldsymbol{\alpha}_5\boldsymbol{\gamma}_2\boldsymbol{\beta}_2}(\mathrm{C}\rightarrow\mathrm{N})$. When viewed along the fivefold axis, the four structures (Figs. 3A–D) resemble a windmill toy, with petal-like protomers. When viewed perpendicular to the fivefold axis, they form a cylinder, with a diameter of about 75 Å. The diameter of the central hole is about 15 Å, between side chains. In the four heteropentamers the only subunit contacts are dimer interfaces. These features provide a proper structural foundation for the ion-pumping mechanism [29,30]. The computed $\overrightarrow{\boldsymbol{\alpha}_1\boldsymbol{\beta}_2\boldsymbol{\alpha}_1\boldsymbol{\gamma}_2\boldsymbol{\beta}_2}(\mathrm{C}\rightarrow\mathrm{N})$ molecule contains 1122 residues, 18,222 atoms, and 571 hydrogen bonds; $\overrightarrow{\boldsymbol{\alpha}_2\boldsymbol{\beta}_2\boldsymbol{\alpha}_2\boldsymbol{\gamma}_2\boldsymbol{\beta}_2}(\mathrm{C}\rightarrow\mathrm{N})$ contains 1120 residues, 19,287 atoms, and 559 hydrogen bonds; $\overrightarrow{\boldsymbol{\alpha}_3\boldsymbol{\beta}_2\boldsymbol{\alpha}_3\boldsymbol{\gamma}_2\boldsymbol{\beta}_2}(\mathrm{C}\rightarrow\mathrm{N})$ contains 1170 residues, 19,036 atoms, and 658 hydrogen bonds; and $\overrightarrow{\boldsymbol{\alpha}_5\boldsymbol{\beta}_2\boldsymbol{\alpha}_5\boldsymbol{\gamma}_2\boldsymbol{\beta}_2}(\mathrm{C}\rightarrow\mathrm{N})$ contains 1128 residues, 18,282 atoms, and 555 hydrogen bonds. The following three criterions were used to test the predicted structures. Let us first consider the structure $\overrightarrow{\boldsymbol{\alpha}_1\boldsymbol{\beta}_2\boldsymbol{\alpha}_1\boldsymbol{\gamma}_2\boldsymbol{\beta}_2}(\mathrm{C}\rightarrow\mathrm{N})$.

(1) *Disulfide bonds.* A hallmark of the ligand-gated pentameric channels is the existence of a disulfide bond in each of its subunits at the N-terminal. This is exactly true as for $\overrightarrow{\boldsymbol{\alpha}_1\boldsymbol{\beta}_2\boldsymbol{\alpha}_1\boldsymbol{\gamma}_2\boldsymbol{\beta}_2}(\mathrm{C}\rightarrow\mathrm{N})$ as shown by the ball-and-stick drawing in Fig. 3A. According to the predicted model, the α_1 subunit is with a disulfide bond

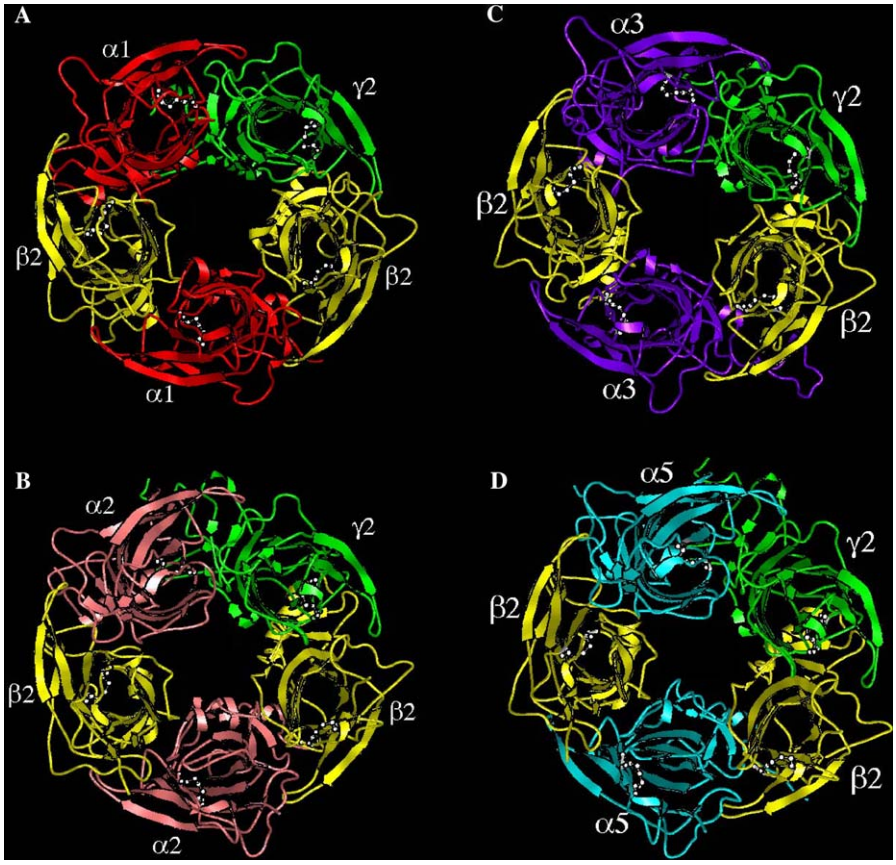

Fig. 3. The computed structure of GABA-A receptor (viewed from C- to N-terminal) for (A) subtype 1, (B) subtype 2, (C) subtype 3, and (D) subtype 5, where α_1 subunit is in red, α_2 in pink, α_3 in purple, α_5 in light blue, β_2 in yellow, and γ_2 in green. The Cys pair involved in forming disulfide bond is depicted by white ball-and-stick drawing. (For interpretation of the references to colour in this figure legend, the reader is referred to the web version of this paper.)

between Cys166 and Cys180, β_2 subunit with a disulfide bond between Cys160 and Cys174, and γ_2 with a disulfide bond between Cys190 and Cys204.

(2) α_1/β_2 *interface.* As is well known, the GABA molecule first docks into α_1/β_2 interface, leading to an allosteric conformational change and increasing the ion flow through the channel and the affinity of diazepam to the α_1/γ_2 interface. The ion flow is called GABA-induced chloride current or GABA current. Moreover, the binding of diazepam will further increase the affinity of GABA to the α_1/β_2 interface, implying that the whole process is a positive cooperative one [5,7,31,32]. Mutational studies [5,6,31] have shown that the key residues to GABA affinity are α_1-Phe92, α_1-Arg147 and β_2-Tyr181, β_2-Thr184, β_2-Thr226, β_2-Tyr229, suggesting that such six residues must be grouped around the α_1/β_2 interface. The predicted structure for $\overrightarrow{\alpha_1\beta_2\alpha_1\gamma_2\beta_2}$ (C → N) indeed indicates so, as shown in Fig. 4A. Meanwhile, it has been found that the area of the surface buried into the interface between α_1 and β_2 subunits is 1235 Å^2.

(3) α_1/γ_2 *interface.* It is known that the benzodiazepine binding site of GABA-A receptors is located in the α_1/γ_2 interface (see, e.g., [5]). Furthermore, a series of experimental observations through binding and functional studies indicate that α_1-His129, α_1-Tyr-187, α_1-Gly228, α_1-Thr234, α_1-Tyr237, and γ_2-Met96, γ_2-Phe116, γ_2-Ser130, γ_2-Gly143, and γ_2-Met169 are important either to the binding of benzodiazepine or to the function of stimulating GABA currents by ligands of the benzodiazepine binding site [5,6,31], suggesting that these residues should be grouped around the α_1/γ_2 interface. Again, the predicted structure does indicate so, as shown in Fig. 4B. Also, it has been found that the area of the surface buried into the interface between α_1 and γ_2 subunits is 1114 Å^2.

The above results have indicated that the predicted structure for $\overrightarrow{\alpha_1\beta_2\alpha_1\gamma_2\beta_2}$(C → N) is completely consistent with all the relevant experimental results known so far. Likewise, the same was true by following the above three examination procedures for the structures $\overrightarrow{\alpha_2\beta_2\alpha_2\gamma_2\beta_2}$(C → N) (Fig. 3B), $\overrightarrow{\alpha_3\beta_2\alpha_3\gamma_2\beta_2}$(C → N) (Fig. 3C), and $\overrightarrow{\alpha_5\beta_2\alpha_5\gamma_2\beta_2}$(C → N) (Fig. 3D), respectively.

However, if the criteria (2) and (3) were used to examine the structures of Eq. (4), i.e., $\overrightarrow{\alpha_1\beta_2\alpha_1\gamma_2\beta_2}$ (C → N), $\overrightarrow{\alpha_2\beta_2\alpha_2\gamma_2\beta_2}$(C → N), $\overrightarrow{\alpha_3\beta_2\alpha_3\gamma_2\beta_2}$ (C → N), and $\overrightarrow{\alpha_5\beta_2\alpha_5\gamma_2\beta_2}$(C → N), it was found that those residues which should be grouped around $\alpha_{1,2,3,5}/\beta_2$ interfaces were instead grouped around $\alpha_{1,2,3,5}/\gamma_2$ and β_2/γ_2 interfaces, and that those residues which should be grouped around $\alpha_{1,2,3,5}/\gamma_2$ interfaces were grouped around $\alpha_{1,2,3,5}/\beta_2$ and γ_2/β_2 interfaces. Accordingly, the structures as formulated in Eq. (4) are not consistent with the experimental observations and hence will be dropped for further consideration. Also, this has clarified the ambiguity about the two possible arrangements of the five subunits in GABA-receptors that could not be uniquely determined by the existing experiment data. In other words, the subtypes 1, 2, 3, and 5 of GABA-A receptors should be formulated by $\overrightarrow{\alpha_1\beta_2\alpha_1\gamma_2\beta_2}$(C → N), $\overrightarrow{\alpha_2\beta_2\alpha_2\gamma_2\beta_2}$(C → N), $\overrightarrow{\alpha_3\beta_2\alpha_3\gamma_2\beta_2}$ (C → N), and $\overrightarrow{\alpha_5\beta_2\alpha_5\gamma_2\beta_2}$(C → N), respectively.

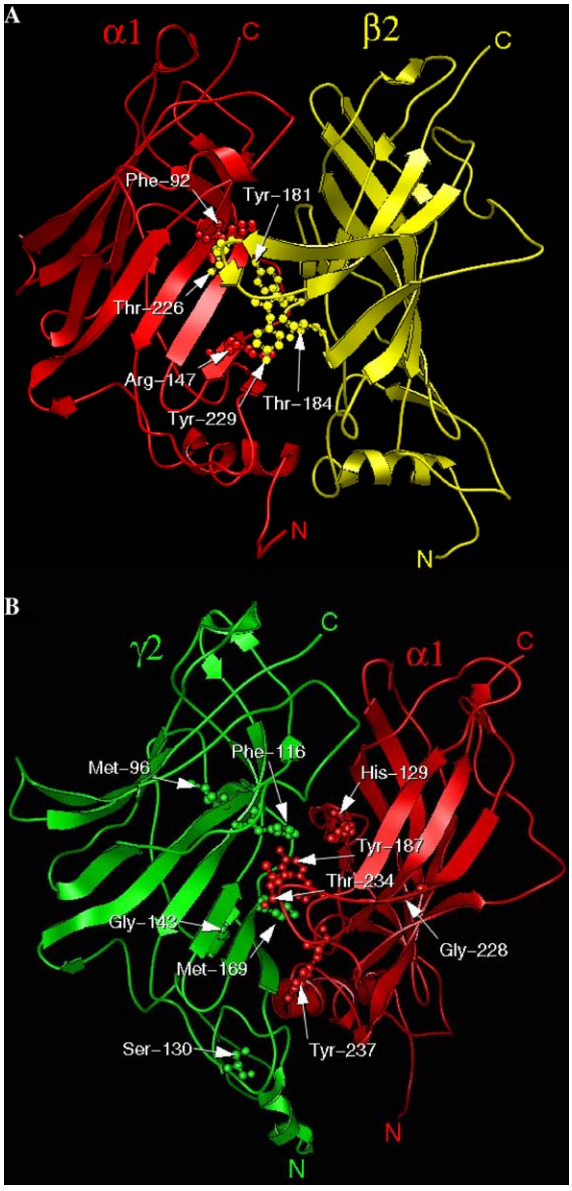

Fig. 4. A close view to show that (A) α_1-Phe92, α_1-Arg147, and β_2-Tyr181, β_2-Thr184, β_2-Thr226, β_2-Tyr229 are grouped around the α_1/β_2 interface, and that (B) α_1-His129, α_1-Tyr-187, α_1-Gly228, α_1-Thr234, α_1-Tyr237, and γ_2-Met96, γ_2-Phe116, γ_2-Ser130, γ_2-Gly143, γ_2-Met169 are grouped around the α_1/γ_2 interface. Both are fully consistent with the experimental observations. See text for further explanation.

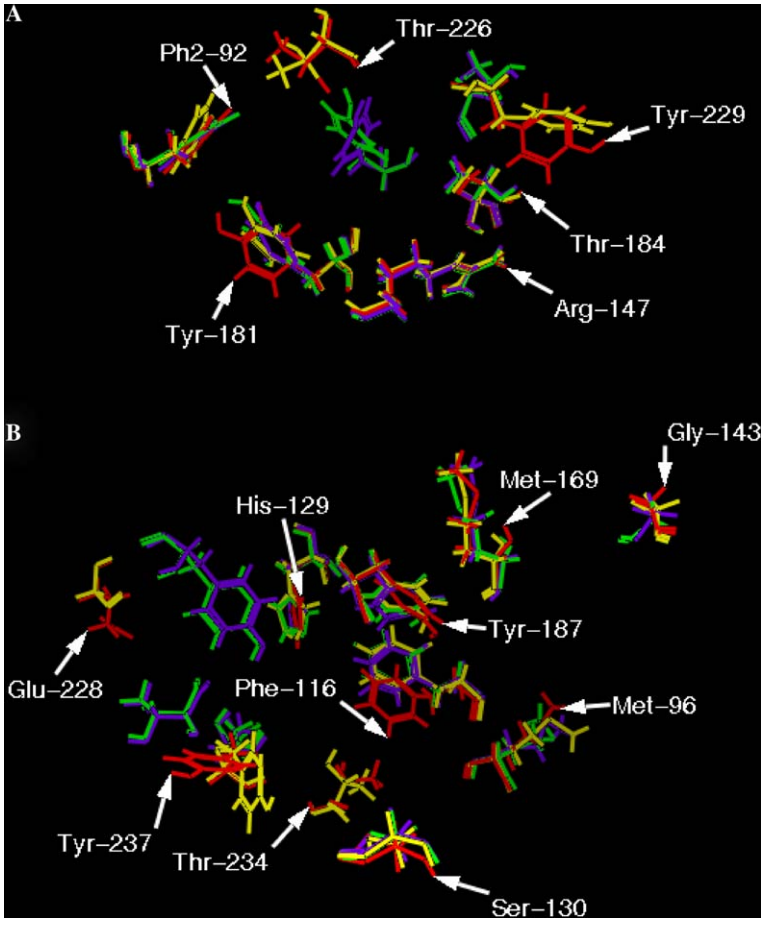

Fig. 5. A structural superposition of the key residues of subtype 2 (red) with those of subtype 1 (yellow), subtype 3 (purple), and subtype 5 (green) to help pinpoint the subtle structural difference around (A) the $\alpha_{1,2,3,5}/\beta_2$ interfaces and (B) the $\alpha_{1,2,3,5}/\gamma_2$ interfaces. See the legends to Figs. 4–5 for further explanation. (For interpretation of the references to colour in this figure legend, the reader is referred to the web version of this paper.)

As far as the constituent subunits are concerned, the only difference among subtypes 1, 2, 3, and 5 is in the α subunit. The sequence identity of α_2 with α_1, α_3, or α_5 subunit is 81%, 81%, or 78%, respectively (Fig. 2). Therefore, the overall structure of subtype 2 (Fig. 3B) looks almost the same as those of subtype 1 (Fig. 3A), subtype 3 (Fig. 3C), and subtype 5 (Fig. 3D). Nevertheless, there is some subtle difference among the four structures that might be important for designing drugs with subtype 2 selectivity. To provide a close look at the difference, a structural superposition of the aforementioned key residues in the four subtypes of GABA-A receptors is presented in Fig. 5, where panel (a) is for those regarding $\alpha_{1,2,3,5}/\beta_2$ interface and panel (b) for those regarding $\alpha_{1,2,3,5}/\gamma_2$ interface.

Conclusion

GABAergic inhibition has become one of the most rapidly developing topics in neuropharmacology. To stimulate the structure-based design of highly selective drugs in this area, the 3D structures of the extracellular domains of subtypes 1, 2, 3, and 5 of GABA-A receptors have been derived. A comparison with various experimental observations has indicated that the predicted structures are quite consistent with the existing data known so far. Furthermore, the predicted structures have clarified some ambiguities that could not beensolved by the existing experimental data, such as the arrangement order of the subunits in the heteropentamers. Expressed in terms of the symbols introduced in the current paper, the stoichiometry and arrangement of the five subunits for subtypes 1, 2, 3, and 5 of GABA-A receptors should be $\overrightarrow{\alpha_1\beta_2\alpha_1\gamma_2\beta_2}$ $(C \to N)$, $\overrightarrow{\alpha_2\beta_2\alpha_2\gamma_2\beta_2}(C \to N)$, $\overrightarrow{\alpha_3\beta_2\alpha_3\gamma_2\beta_2}(C \to N)$, and $\overrightarrow{\alpha_5\beta_2\alpha_5\gamma_2\beta_2}$ $(C \to N)$ of Eq. (3), respectively, but not their mirror images of Eq. (4). Since GABA is a common therapeutic target for the treatment of CNS diseases, the current models may serve as a reasonable 3D structural frame for conducting mutagenesis and docking studies, providing insights or stimulating development of novel strategies for designing highly selective drugs for CNS

diseases such as generalized anxiety disorders, sleep disturbances, muscle spasms, and seizure disorders.

References

[1] U. Gunther, J. Benson, D. Benke, J.M. Fritschy, G. Reyes, F. Knoflach, F. Crestani, A. Aguzzi, M. Arigoni, Y. Lang, Proc. Natl. Acad. Sci. USA 92 (1995) 7749–7753.

[2] H.A. Wieland, H. Luddens, P.H. Seeburg, J. Biol. Chem. 267 (1992) 1426–1429.

[3] R.M. McKernan, P.J. Whiting, Trends Neurosci. 19 (1996) 139–143.

[4] H. Mohler, J.M. Fritschy, U. Rudolph, J. Pharmacol. Exp. Ther. 300 (2002) 2–8.

[5] E. Sigel, A. Buhr, Trends Pharmacol. Sci. 18 (1997) 425–429.

[6] T. Klausberger, K. Fuchs, B. Mayer, N. Ehya, W. Sieghart, J. Biol. Chem. 275 (2000) 8921–8928.

[7] S.W. Baumann, R. Baur, E. Sigel, J. Biol. Chem. 276 (2001) 36275–36280.

[8] V. Tretter, N. Ehya, K. Fuchs, W. Sieghart, J. Neurosci. 17 (1997) 2728–2737.

[9] P.R. Schofield, D.B. Pritchett, H. Sontheimer, H. Kettenmann, P.H. Seeburg, FEBS Lett. 244 (1989) 361–364.

[10] P. Wingrove, K. Hadingham, K. Wafford, J.A. Kemp, C.I. Ragan, P. Whiting, Biochem. Soc. Trans. 20 (1992) 18S.

[11] K.L. Hadingham, P. Wingrove, B. Le Bourdelles, K.J. Palmer, C.I. Ragan, P.J. Whiting, Mol. pharmacol. 43 (1993) 970–975.

[12] D.D. McKinley, D.J. Lennon, D.B. Carter, Brain Res. Mol. Brain Res. 28 (1995) 175–179.

[13] D.B. Pritchett, H. Sontheimer, B.D. Shivers, S. Ymer, H. Kettenmann, P.R. Schofield, P.H. Seeburg, Nature 338 (1989) 582–585.

[14] J.D. Thompson, D.G. Higgins, T.J. Gibson, Nucleic Acids Res. 22 (1994) 4673–4680.

[15] K.C. Chou, Curr. Protein Peptide Sci. 3 (2002) 615–622.

[16] K.C. Chou, Protein Eng. 14 (2001) 75–79.

[17] K. Brejc, W.J. van Dijk, R.V. Klaassen, M. Schuurmans, J. van der Oost, A.B. Smit, T.K. Sixma, Nature 411 (2001) 269–276.

[18] T.A. Jones, S. Thirup, EMBO J. 5 (1986) 819–822.

[19] T.L. Blundell, B.L. Sibanda, M.J.E. Sternberg, J.M. Thornton, Nature (London) 326 (1987) 347–352.

[20] K.C. Chou, G. Nemethy, M. Pottle, H.A. Scheraga, J. Mol. Biol. 205 (1989) 241–249.

[21] B.C. Finzel, S. Kimatian, D.H. Ohlendorf, J.J. Wendoloski, M. Levitt, F.R. Salemme, in: C.E. Bugg, S.E. Ealick (Eds.), Crystallographic and Modeling Methods in Molecular Design, Springer-Verlag, Berlin, 1989, pp. 175–188.

[22] M. Levitt, J. Mol. Biol. 226 (1992) 507–533.

[23] K.C. Chou, D. Jones, R.L. Heinrikson, FEBS Lett. 419 (1997) 49–54.

[24] W. Watt, K.A. Koeplinger, A.M. Mildner, R.L. Heinrikson, A.G. Tomasselli, K.D. Watenpaugh, Structure 7 (1999) 1135–1143.

[25] J.J. Chou, H. Matsuo, H. Duan, G. Wagner, Cell 94 (1998) 171–180.

[26] K.C. Chou, K.D. Watenpaugh, R.L. Heinrikson, Biochem. Biophys. Res. Commun. 259 (1999) 420–428.

[27] K.C. Chou, A.G. Tomasselli, R.L. Heinrikson, FEBS Lett. 470 (2000) 249–256.

[28] K.C. Chou, W.J. Howe, Biochem. Biophys. Res. Commun. 292 (2002) 702–708.

[29] K.C. Chou, J. Protein Chem. 12 (1993) 337–350.

[30] K.C. Chou, Amino Acids 7 (1994) 1–17.

[31] A. Buhr, E. Sigel, Proc. Natl. Acad. Sci. USA 94 (1997) 8824–8829.

[32] S. Renard, A. Olivier, P. Granger, P. Avenet, D. Graham, M. Sevrin, P. George, F. Besnard, J. Biol. Chem. 274 (1999) 13370–13374.